Title: CXCL-8/IL-8 produced by diffuse large B-cell lymphomas recruits neutrophils expressing a proliferation inducing ligand APRIL.
Authors: Manfroi B, McKee T, Mayol JF, Tabruyn S, Moret S, Villiers C, Righini C, Dyer M, Callanan M, Schneider P, Tzankov A, Matthes T, Sturm N, Huard B
Journal: Cancer research
Year: 2016 Dec 6
DOI: 10.1158/0008-5472.CAN-16-0786

CXCL-8/IL-8 produced by diffuse large B-cell lymphomas recruits neutrophils expressing a proliferation inducing ligand APRIL

Manfroi B.[1], McKee T.[2], Mayol J.F.[3], Tabruyn S.[3], Moret S.[4], Villiers C. [1], Righini C.[5], Dyer M.[6], Callanan M.[1], Schneider P.[8], Tzankov A.[9], Matthes T.[10], Sturm N.[1,7] and Huard B.[1]

[1] Albert Bonniot Institute, INSERM U1209/University Grenoble-Alpes, La Tronche, France.
[2] Clinical Pathology, University Hospital of Geneva, Switzerland.
[3] Transcure Biosciences, Archamps Biopark, France.
[4] Department of Pathology-Immunology, Geneva University Medical Centre, Switzerland
[5] Head and Neck Department, Grenoble University Hospital, France.
[6] Ernest and Helen Scott Hematological Research Institute, University of Leicester, UK
[7] Department of Anatomy and Cytopathology, University Hospital of Grenoble, France
[8] Department of Biochemistry, University of Lausanne, Epalinges, Switzerland
[9] Institute of Pathology, University Hospital Basel, Basel, Switzerland
[10] Hematology, University Hospital of Geneva, Switzerland.

Corresponding author:
Bertrand Huard
Bertrand.huard@univ-grenoble-alpes.fr
+33476549447

Running title: neutrophils in B-cell lymphoma

Keywords: B-cell lymphoma, Inflammation, Tumor-associated neutrophils, chemokines

Acknowledgements:

The Leenaards Foundation, the INSERM, the university Grenoble Alpes, the ligue contre le cancer (committee 38), and the region Auvergne/Rhone-Alpes supported this work. PS is supported by the Swiss National Science Foundation.

PS is supported by a research grant from Merck EMD, a subsidiary of Merck, KGaA. Other authors declare no competing financial interest.

Tumor infiltrating neutrophils have been implicated in malignant development and progression but mechanisms are ill-defined. Neutrophils produce a proliferation-inducing ligand APRIL/TNFSF13, a factor that promotes development of tumors from diverse origins, including diffuse large B-cell lymphoma (DLBCL). High APRIL expression in DLBCL correlates with reduced patient survival, but the pathway(s) dictating APRIL expression are not known. Here we show that all blood neutrophils constitutively secrete APRIL, and inflammation-associated stimuli such as TNF further upregulate APRIL. In a significant fraction of DLBCL patients tumor cells constitutively produced the ELC-CXC chemokine CXCL-8 (IL-8), enabling them to recruit APRIL-producing blood neutrophils. CXCL-8 production in DLBCL was unrelated to the cell of origin, as APRIL-producing neutrophils infiltrated CXCL-8+ DLBCL from both germinal center (GC) and non-GC subtypes. Rather, CXCL-8 production implied events affecting DNA methylation and acetylation. Overall, our results showed that chemokine-mediated recruitment of neutrophils secreting the tumor-promoting factor APRIL mediates DLBCL progression.

Introduction

The microenvironment is a key player in tumor development (1). Tumor microenvironment comprises stromal cells and endothelial cells. When tumor development is associated to a host inflammatory reaction, infiltrating leukocytes from the blood become also part of the microenvironment. Myeloid cells often infiltrate tumors, and their pro or anti-tumoral role, especially with macrophages, has been extensively studied (2, 3).

In addition to the well-described role for macrophages, a role for neutrophils in the development of tumors has been recently proposed (4). Neutrophils have been reported to increase cancer genetic instability by their production of nitric oxide derivatives and reactive oxygen species (5), to promote angiogenesis by their secretion of pro-angiogenic factors (6, 7), and also to produce immunosuppressive factors, such as IL-10 (8). For all these reasons, neutrophil infiltration of several solid tumors has been associated with a poorer outcome for patients (9). On the other hand, neutrophils may also act as anti-tumoral immune cells via their expression of the apoptotic ligand TRAIL (10). Furthermore, elastase, a protease commonly secreted by neutrophils, is also an anti-angiogenic factor (11). Hence, the role of neutrophils in tumor development is contrasted, and it is believed that neutrophils may be polarized, in effector cells with either pro- or anti-tumoral function, very similarly to macrophages (12).

Neutrophils produce a proliferation inducing ligand (APRIL, TNFSF13) (13). The initial reported function of APRIL was induction of increased proliferation in tumor cells (14). This role has been further substantiated in colorectal cancers (15). Hematologic tumors from the B-cell lineage also depend on APRIL (16). The best-documented B-cell malignancy depending on APRIL is chronic lymphocytic leukemia (CLL). In CLL, APRIL is of stromal origin, and prolongs the *in vitro* survival of primary CLL samples (17, 18). Furthermore, APRIL overexpression in mice leads to CLL-like neoplasm development. In patients, high APRIL serum level correlates with reduced patient survival (19-22). Regarding DLBCL, APRIL also acts as an *in vitro* survival factor (23), and a high level of APRIL in tumor lesions is a risk factor, at least in patients treated with CHOP chemotherapy (24). While DLBCL tumor cells may aberrantly produced APRIL upon translocations involving the APRIL gene and the immunoglobulin heavy chain locus (25), we previously observed that most of APRIL originates from infiltrating neutrophils (24). Here, we are describing the pathway conducting to high APRIL expression in DLBCL lesions.

Methods

Human and animal experimentations

The Basel and Grenoble ethical committees approved human experimentations. The basel DLBCL cohort has been previously described (26). Frozen DLBCL biopsies and corresponding formalin-fixed paraffin-embedded DLBCL biopsies used for mRNA analysis were obtained after patients' informed consent from the centre of biological resources (Grenoble, France). Two pathologists independently reviewed DLBCL diagnosis. In some cases, GC and non-GC DLBCL subtypes were defined by immunohistochemistry with the combination of CD10, bcl-6 and Mum-1/IRF-4 markers as reported (27). Peripheral blood leukocytes were obtained from healthy donors (French blood institute, Grenoble). The Geneva CELEA ethical committee approved mouse experimentations. Four weeks-old immunodeficient NOG mice (Taconic) were engrafted with cord blood-derived $CD34^+$ hematopoietic stem and progenitor cells (French blood institute) two days after chemical myeloablative treatment. Engraftment consisted in intravenous injection of 10^5 $CD34^+$ cells. Fourteen weeks after cell injection, engraftment level was monitored with the analysis of human $CD45^+$ cells among total blood leukocytes by flow cytometry (Attune, Life technologies). 10^7 tumor cells were injected subcutaneously in mice harboring at least 10% of engraftment level.

Neutrophil stimulation

Neutrophils were purified following standard dextran sedimentation followed by Ficoll-paque centrifugation and FACS-sorting based on FSC^{high} SSC^{high} morphology on a FACS-Aria (BD Biosciences). After purification $CD13^+CD16^+$ neutrophils represented more than 85% and 80%, respectively. Viability assessed by trypan blue staining was > 95% after 24 h. Conditioned supernatants were obtained by incubating neutrophils at 10^6 cells per ml in RPMI 1640 supplemented with 10% heat-inactivated FCS. Cell stimulation was performed with either fMLP (6.10^{-9}M, Sigma) or phorbol 12-myristate 13-acetate (PMA, 50 ng/ml, Sigma) or TNF (100 ng/ml, Adipogen). Cell-free supernatant was analysed for secreted APRIL by ELISA using manufacturer's instructions (eBioscience). Cells were also harvested for APRIL mRNA expression at 6 and 12 h.

For the analysis of H_2O_2 production, 0.5 x 10^6 cells were mixed in a 96-well plate with 20 mM glucose, 20 µM luminol and 10U/ml HRP and with the activators described above. Luminescence was recorded at 37°C every 15 s for 10 min using a Victor3 1420 multilabel counter (Perkin Elmer).

Immunohistochemistry

Biopsies were stained for APRIL-producing cells (Stalk-1 staining), elastase, and CD20 as previously described (24). Rabbit anti-CXCL-8 (Life technologies) was used at 5 µg/ml after heat-induced antigen retrieval in 10 mM Tris, 1 mM EDTA pH 9.0. Microscopy images were visualized with a BX-41 microscope (Olympus) with a plan 40x/0,65 air objective and a plan 100x/1,25 oil objective. Images were captured with a DP70 color camera and treated with the AnalySIS software. Confocal analysis was performed on an LSM 510 microscope (Carl Zeiss) with a plan 40x/1.30 oil-immersion objective.

Flow cytometry

All fluorochrome-conjugated antibodies were from BD biosciences. APRIL staining with Stalk-1 (detecting APRIL-producing cells) was performed after cell permeabilization as previously described (24). Fluorescence was analysed by flow cytometry on a FACS CALIBUR or an Accuri C6 (BD biosciences). $CD20^+$ and $CD20^-$ fraction of frozen primary DLBCL were purified by FACS-sorting on a FACS-Aria (BD biosciences). $CD19^+$ B-cell subsets were purified from tonsils according to naive ($IgD^+/CD38^-$), GC ($CD38^+$) and memory ($IgD^-/CD38^-$) phenotype. Dead cells were excluded by 7-AAD staining. Purity and viability was > 95%.

PCR

For the detection of ELC-CXC chemokine mRNA, 30 sections of 20 µm from frozen DLBCL biopsies were pooled, and total RNA was extracted with the RNeasy micro kit (Qiagen). cDNA was generated using random primers and the SuperScript II reverse transcriptase (Invitrogen). For CXCL-2 5'-ctttccagccccaaccat-3' and 5'-ggatttgccatttttcagca-3', for CXCL-3 5'-cccaaaccgaagtcatagcc-3' and 5'-agttccccaccctgtcattt-3', for CXCL-5 5'-ccaatcttcgctcctccaat-3' and 5'-tccttgtttccaccgtcca-3', for CXCL-6 5'-acccctttctttccacactgc-3' and 5'-ggaggctaccacttccacct-3', for CXCL-8 5'-cggaaggaaccatctcactg-3' and 5'-agcactccttggcaaaactg-

3', for CCL-7 5'-cagaaggaccaccagtagcc-3' and 5'-gcatcccacagtttttacagc-3', for CCL-13 5'-cagaggagcagagaggcaaa-3' and 5'-gccagaggagaatggaaaagtc-3', for CCL-14 5'-gctctcctcccacaacagc-3' and 5'-gccaatgagtaaatcccgtaga-3' were used as forward and reverse primers, respectively. Denaturation was performed at 94°C, annealing at 55°C and extension at 72°C, 1 mn each. Forty cycles were applied. Amplified PCR products were visualized on agarose gels and ethidium bromide staining. To exclude genomic DNA amplification, primers spanning intronic sequences were used.

For quantitative analysis, total RNA was extracted using Trizol (Invitrogen), and cDNA generated as above. Quantification was performed using the iCycler iQ Real-Time PCR Detection system (Bio-Rad) and a SYBRgreen-based kit (iQ SupermixBio-Rad). The intron spanning forward 5'- atgggtcaggtggtgtctcg-3' and reverse 5'- tcccctggtgtaaatggaaga-3' primers were used for the detection of human APRIL. Expression levels were normalized using 18S rRNA. Results were quantified using a standard curve generated with serial dilutions of input DNA.

Chemokine profiling and ELISA

30 sections of 20 µm from frozen DLBCL biopsies were pooled, lyzed in Na phosphate 0.01 M, EDTA 1 mM, EGTA 1mM, NaF 1 mM, NaCl 0.15 M pH=7.2, containing 1 % Triton X-100, 0.1% NaDOC, 1 mM PMSF and complete mini cocktail protease inhibitors from Roche. Protein quantification in lysates was performed with a BCA protein assay kit (Pierce). The human cytokine profiling kit, and CXCL-8 ELISA were from R&D. DLBCL OCI cell lines were provided by M. Minden (Ontario Cancer Institute, Toronto, Canada). Dr A. Wiestner (NIH, Bethesda, MD) provided the Su-DHL cell lines. B593, HT, HBL-1, K422, Nu-DUL-1, Pfeiffer, RC-K8, RIVA, and U2932 have been already described (28, 29). 0.5 x 10^6 DLBCL cells per ml were incubated for 48h for supernatant conditioning. Cell stimulation was performed with an anti-BCR (goat anti-human Ig, 1 µg/ml, Life Technologies), Fc-CD40L (1 µg/ml, Enzo Life Sciences) and TNF (100 ng/ml, Adipogen).

Chemotactism assay

DLBCL cells were incubated in bottom compartments of a 8-µM 24-transwell plate (Nunc) at 0.5 x 10^6 cells per ml. 72 h later, 0.2 x 10^6 purified neutrophils were added in upper

compartments. Rabbit anti CXCL-8 (Life Technologies) was used at 10 µg/ml. After 2 h incubation, neutrophils in bottom wells were stained with an anti-CD13 and CD16, and numerated by flow cytometry with an Accurri C6 set on a volume-based event acquisition.

Epigenetic studies

0.5 x 10^6 DLBCL cells per ml were incubated for 24 h with Trichostatin A (TSA, 500 ng/ml, Sigma) or 72 h with Decitabine (10 µM, Sigma). DMSO was used as a vehicle control. Real time RT-PCR was performed as described above with forward and reverse primers for CXCL-8 5'-cggaaggaaccatctcactg-3' and 5'-agcactccttggcaaaactg-3', respectively. Expression levels were normalized using actin mRNA. Results were quantified using a standard curve generated with serial dilutions of input DNA.

Statistics

Data are presented as means ± s.d. Statistical analyses were performed with two-tailed unpaired Mann-Whitney U test on samples of equal size using the Prism software (Graphpad Software Inc., San Diego, CA, USA). *P*-values superior to 0.05 were considered as non-significant.

Results

Blood neutrophils constitutively produce APRIL

Neutrophils usually produce their effector proteins at an immature stage and store these proteins in intracellular granules to release them upon activation at the inflammation site (30). Transcription of neutrophil effector proteins is commonly stopped at neutrophil maturity. We previously reported that APRIL production is also switched on early in immature neutrophils, but APRIL transcription drops by two third but does not stop in mature neutrophils, at least for mature neutrophils present in bone marrow (BM) (31). In the blood circulation, APRIL transcription in neutrophils did not stop as well, and was equal to that in mature neutrophils from BM (figure 1A, left panel). All blood neutrophils were reactive with Stalk-1, an antibody against APRIL identifying APRIL-producing cells (figure 1A, middle panel). We further observed constitutive APRIL secretion in 24h culture supernatants of neutrophils purified by sedimentation and FACS sorting according to morphology (figure 1A, right panel). The common activators

PMA, TNF and fMLP rapidly induced H_2O_2 release, a marker of neutrophil activation, from blood mature neutrophils (figure 1B, top left panel). However, only PMA and to a lesser extent TNF upregulated APRIL transcription (figure 1B, top right panel). Upregulation of APRIL transcription correlated with a concomitant increased accumulation of secreted APRIL in the supernatant (figure 1B, bottom panel). This argued against APRIL storage in neutrophils. Taken together, these results showed that APRIL secretion in neutrophils is constitutive and further upregulated by inflammatory stimuli.

DLBCL tumor cells variably express the chemokine CXCL-8

The mechanism by which APRIL production varies in DLBCL lesions is presently unknown. Our previous work indicated that infiltrating neutrophils are a cellular source of APRIL in DLBCL lesions (24). Among APRIL^{high} DLBCL cases, we are now reporting a significant infiltration (mean = 25 per mm^2, range 4-318) of neutrophils in about 75% of these cases (n=101). The demonstration that blood neutrophils constitutively produced APRIL indicates that variation of APRIL expression may originate from a differential neutrophil recruitment in tumor lesions. We selected representative APRIL^{neg} and APRIL^{high} patients, with the latter being infiltrated by elastase$^+$ neutrophil producing APRIL (figure 2a, upper and middle panels). We profiled chemokine expression in lysates of frozen biopsies from these two patients. CXCL-8 was upregulated in the APRIL^{high} neutrophil^{high} patient (figure 2A, bottom left panel). CXCL-8 is one ligand of CXCR-2 known as the main driver of neutrophil migration (32), but other chemokines may act on neutrophils (33). The neutrophil-specific chemokines CXCL-1, -12 and CCL-2, -3, -4, -5 were not upregulated on the blot, and the remaining neutrophil-specific chemokines CXCL-2, -3, -5, -6 and CCL-7, -13, -14 were not detectable at the mRNA level in this patient (figure 1 sup). An ELISA confirmed the upregulation of CXCL-8 in lysates of 3 non-necrotic DLBCL biopsies from APRIL^{high} patients (figure 2B). *In situ* staining with an anti-CXCL-8 showed intracellular staining in cells harboring large central single nucleolus, reminiscent of immunoblastic DLBCL tumor cells (figure 2C). Costaining experiments confirmed that CXCL-8 was indeed present in the cytoplasm of CD20$^+$ DLBCL tumor cells in lesions infiltrated by neutrophils but not in non-infiltrated lesions (figure 2D). We confirmed specific CXCL-8 expression by tumor cells at the mRNA level in CD20$^+$ fraction of primary DLBCL but not in CD20$^-$ cells (Figure 2E). In this experiment, we did not detect CXCL-8

mRNA in $CD20^+$ DLBCL tumor cells from non-infiltrated lesions. In these samples, Finally, CXCL-8 secretion was detected in the supernatant of CD20+ fraction of primary DLBCL from $APRIL^{high}$ patients cultured for 3 days (mean = 175 pg/ml, range 30.42 – 445.27 pg/ml, n=3). In total, we observed CXCL-8 immunostaining in 95% of the case infiltrated by neutrophils. CXCL-8 protein expression was undetectable in 90% of the $APRIL^{neg}$ patients. These neutrophils infiltrated the tumor nest, in close vicinity with tumor cells (figure 2 sup). Tumoral necrotic cells were found in 30% of cases infiltrated by neutrophils (figure 3A sup). CXCL-8 production by neutrophils was found in 12% of infiltrated cases and was always associated with necrosis (figure 3B sup). However, CXCL-8 production by neutrophils was never observed in non-necrotic cases. Finally, we also detected CXCL-8 in the supernatant of 11 of 24 DLBCL cell lines (figure 2F). In these 11 cell lines, CXCL-8 secretion was constitutive, and was not related to the cell of origin, since detected in the supernatant of both ABC-like (n=4) and GC-like (n=7) DLBCL subtypes. TNF and anti-BCR/CD40L never induced CXCL-8 secretion in DLBCL cell lines, but anti-BCR/CD40L upregulated CXCL-8 secretion in 7 of the 11 $CXCL\text{-}8^+$ cell lines. Taken together, our data show that some DLBCL tumor cells constitutively produce CXCL-8. A cognate T/B collaboration pathway, mimicked by anti-BCR/CD40L stimulation, may further upregulate this production.

CXCL-8 recruits APRIL-producing neutrophils in DLBCL lesions

In vitro $CXCL\text{-}8^+$ DLBCL cell lines attracted significantly more neutrophils in a standard Boyden chamber assay than $CXCL\text{-}8^-$ DLBCL cell lines (figure 3A). Antibody-mediated inhibition showed the CXCL-8 dependent chemotactic activity of OCI-Ly18, the DLBCL cell line producing the most of CXCL-8 (see figure 2E), and the most efficient to *in vitro* recruit neutrophils (figure 3B). Expression of the two CXCL-8 receptors, CXCR-1 and -2, on the surface of blood mature neutrophils explained their chemotactic response to $CXCL\text{-}8^+$ DLBCL cell lines (figure 3C). CXCL-8 has no murine ortholog, and human CXCL-8 does not efficiently cross-react on mouse neutrophils (34). To demonstrate an *in vivo* chemotactic activity, we used humanized NOG immunodeficient mice. $CD45^{int}CD16^+CD13^+$ mature neutrophils of human origin produced APRIL in BM of these mice (figure 4A). We further observed the presence of APRIL-producing cells harboring a nuclear morphology reminiscent of neutrophils, selectively infiltrating the $CXCL\text{-}8^+$ OCI-Ly18 tumor xenografts made in these mice (figure 4B). These

APRIL-producing infiltrating cells were indeed neutrophils expressing elastase (figure 4C). This xenogeneic model reproduced the situation in patients in terms of expression pattern with all cells producing APRIL, and in terms of infiltration level with a mean of 55 cells per mm^2, range 33-143, n=3. Taken together, our data show that CXCL-8, produced by DLBCL tumor cells, efficiently recruits blood neutrophils.

CXCL-8 production in DLBCL is a post-transformation event

Among the 11 CXCL-8^+ DLBCL cell lines, bcl-2 expression was detected in 7 of them. All the cell lines expressed the B-cell marker CD19, except one. All of them expressed HLA-DR. All cell lines differentially expressed CD27 and CD38, and 4 cell lines had undergone a switch IgG^+/IgM^- surface phenotype (figure 5a). Taken together, this revealed a wide heterogeneity in CXCL-8^+ DLBCL. We neither observed CXCL-8 protein expression by immunohistochemistry in healthy GC B cells from tonsil nor CXCL-8 mRNA expression in $CD19^+$ IgD^+ $CD38^-$ naive, $CD19^+$ $CD38^+$ GC and $CD19^+$ IgD^- $CD38^-$ memory B cells (figure 5B, figure 4 sup). This shows that CXCL-8 induction in DLBCL is a post-tranformation event. In DLBCL patients, as in cell lines, CXCL-8 expression was not dependent on the cell of origin, since we detected $APRIL^{high}$ $neutrophil^{high}$ phenotype in GC (n=31) and in non-GC subtypes (n=37). To gain insight into the pathway regulating CXCL-8 expression in DLBCL tumor cells, we performed DNA methylation inhibition with decitabine and upregulation of histone acetylation by histone deacetylase inhibition with trichostatin A (TSA) on a panel of 6 DLBCL cell lines CXCL-8^+ and 6 DLBCL cell lines CXCL-8^-. We applied decitabine and TSA for 3 days and 1 day, respectively. The higher toxicity of TSA on DLBCL cell lines explained the shortened incubation period with this reagent. Decitabine modulated positively CXCL-8 transcription in all DLBCL cell lines tested, with either an upregulation in CXCL-8^+ cell lines, or induction of a detectable transcription in the other cell lines (figure 6A). TSA behaved very similarly with either upregulation or induction of CXCL-8 transcription. At the protein level, decitabine treatment increased CXCL-8 secretion in all the CXCL-8^+ cell lines, and resulted in the faint detection of CXCL-8 in the supernatant of two CXCL-8^- cell lines (figure 6B). We did not detect an increase in CXCL-8 protein level in cell supernatant after TSA treatment. This may be either due to the shorter time treatment or the sensitivity of CXCL-8 transport to histone deacetylases, as described for other proteins (35). Taken together, these experiments showed that the CXCL-8^- DLBCL cell lines tested here still

contain a functional CXCL-8 locus, and this locus is kept silent by DNA methylation and histone hypoacetylation.

Discussion

In the present study, we observed a constitutive production of APRIL by blood circulating neutrophils. These cells do not store APRIL in exocytosis granules but rather constantly secrete it, resulting in a detectable accumulation of APRIL in neutrophil cell culture supernatants. Such secretion pattern by blood neutrophils may explain the steady state concentration in the ng/ml range reported for this cytokine in blood from healthy donors (36-38). Here, we show that blood neutrophils quite frequently infiltrate DLBCL, providing APRIL in DLBCL lesions. Such neutrophil infiltration is due to the constitutive production of CXCL-8 by tumor cells. We did not obtain evidences for the involvement of another chemokine involved. CXCL-8-producing DLBCLs are phenotypically heterogeneous, being either of the GC or the non-GC subtypes. By contrast, healthy GC B cells did not express CXCL-8. Rather, we show that epigenetic events leading to DNA demethylation and/or histone hyperacetylation induce CXCL-8 production by DLBCL. It is known that DLBCL are highly perturbated in their epigenome (39). These perturbations are variable among patients (40). Our present study indicates that epigenetic variations concern CXCL-8. The CXCL-8 gene is derepressable by DNA demethylation and histone hyperacetylation (41). The activation-induced cytidine deaminase (AID) strictly expressed in B cells from GC to mediate somatic hypermutations and class switching also induces DNA demethylation that derepress many genes in GC B cells (42). Derepression of CXCL-8 by DNA demethylation may either occur at that stage or in a post transformation event, considering the fact that AID remains active in DLBCL (43). Variation in histone acetylation is also a hallmark of DLBCL (44). Indeed, DLBCL frequently harbors inactivating mutations in the histone acetyl transferases CREB-binding protein (CREBBP) and p300 (45, 46). Thus, CXCL-8^{+} DLBCLs may represent tumor cells with a still active acetyl transferase activity. Taken together, these processes explain the variable presence of the tumor-promoting APRIL in DLBCL lesions. It is further interesting to note that CXCL-8 production may be amplified *in situ*. Indeed, an anti-BCR/CD40L stimulus, which can be considered as an *in vitro* mimick of a cognate T-helper/B cell interaction increases CXCL-8 production by tumor cells. This latter effect is likely due to an

increase in AID and CREBBP/p300 expression by CD40 signaling (47, 48). To our knowledge, a BCR signalling did not result in the upregulation of these enzymes. CD40 signaling in DLBCL may occur *in situ* own to the frequent infiltration of T-helper cells in tumor lesions (49, 50). Levels of APRIL expression may even be further amplified *in situ* by TNF, a cytokine present in DLBCL lesions (51), and shown here to upregulate APRIL production by neutrophils.

CXCL-8 production by tumor cells including colon, ovarian, prostate and bladder cancers has already been reported (52-55). It is believed that CXCL-8 promotes tumor development, when tumors aberrantly express CXCL-8 receptors, resulting in an autocrine stimulation loop (56). The CXCL-8 tumor-promoting pathway we are demonstrating here is different. Indeed, in DLBCL, CXCL-8 exerts a paracrine loop. Our present results are consistent with a recent report showing that a direct contact between tumor cells and neutrophils enhances in a BAFF/APRIL dependent manner the *in vitro* survival of DLBCL cell lines and primary cultures (57). Regarding CXCL-8 expression in DLBCL, mRNA and tissue protein reactivities have already been reported, but the cellular source was not identified (58). Consistent with our study is the report that high CXCL-8 concentration is associated to an impaired response to chemotherapy (59). Taken together, tumor-derived CXCL-8 promotes neutrophil infiltration, thereby providing a source of the DLBCL-promoting factor APRIL. Such neutrophil infiltration may thus accelerate DLBCL development.

Author Contributions:

BM, SM, CV performed research. JFM, ST made experiments with humanized mice. PS provided APRIL specific reagents. DM and CM provided cell lines. AT, TM, TMcK, JG, NS provided DLBCL biopsies and when available associated clinical data. CR provided tonsils biopises. TMcK and NS performed immunohistochemistry analysis. BM and BH analysed the data. BH designed the study and wrote the manuscript.

REFERENCES

1. Hanahan D, Weinberg RA. Hallmarks of cancer: the next generation. Cell. 2011;144(5):646-74.
2. Porta C, Riboldi E, Totaro MG, Strauss L, Sica A, Mantovani A. Macrophages in cancer and infectious diseases: the 'good' and the 'bad'. Immunotherapy. 2011;3(10):1185-202.

3. Allavena P, Sica A, Garlanda C, Mantovani A. The Yin-Yang of tumor-associated macrophages in neoplastic progression and immune surveillance. Immunol Rev. 2008;222:155-61.
4. Galdiero MR, Bonavita E, Barajon I, Garlanda C, Mantovani A, Jaillon S. Tumor associated macrophages and neutrophils in cancer. Immunobiology. 2013;218(11):1402-10.
5. Gungor N, Knaapen AM, Munnia A, Peluso M, Haenen GR, Chiu RK, et al. Genotoxic effects of neutrophils and hypochlorous acid. Mutagenesis. 2010;25(2):149-54.
6. Scapini P, Morini M, Tecchio C, Minghelli S, Di Carlo E, Tanghetti E, et al. CXCL1/macrophage inflammatory protein-2-induced angiogenesis in vivo is mediated by neutrophil-derived vascular endothelial growth factor-A. J Immunol. 2004;172(8):5034-40.
7. Scapini P, Nesi L, Morini M, Tanghetti E, Belleri M, Noonan D, et al. Generation of biologically active angiostatin kringle 1-3 by activated human neutrophils. J Immunol. 2002;168(11):5798-804.
8. De Santo C, Arscott R, Booth S, Karydis I, Jones M, Asher R, et al. Invariant NKT cells modulate the suppressive activity of IL-10-secreting neutrophils differentiated with serum amyloid A. Nat Immunol. 2010;11(11):1039-46.
9. Shen M, Hu P, Donskov F, Wang G, Liu Q, Du J. Tumor-associated neutrophils as a new prognostic factor in cancer: a systematic review and meta-analysis. PLoS One. 2014;9(6):e98259.
10. Cassatella MA. On the production of TNF-related apoptosis-inducing ligand (TRAIL/Apo-2L) by human neutrophils. J Leukoc Biol. 2006;79(6):1140-9.
11. Ai S, Cheng XW, Inoue A, Nakamura K, Okumura K, Iguchi A, et al. Angiogenic activity of bFGF and VEGF suppressed by proteolytic cleavage by neutrophil elastase. Biochem Biophys Res Commun. 2007;364(2):395-401.
12. Fridlender ZG, Albelda SM. Tumor-associated neutrophils: friend or foe? Carcinogenesis. 2012;33(5):949-55.
13. Tecchio C, Scapini P, Pizzolo G, Cassatella MA. On the cytokines produced by human neutrophils in tumors. Semin Cancer Biol. 2013;23(3):159-70.
14. Hahne M, Kataoka T, Schroter M, Hofmann K, Irmler M, Bodmer JL, et al. APRIL, a new ligand of the tumor necrosis factor family, stimulates tumor cell growth. J Exp Med. 1998;188(6):1185-90.
15. Lascano V, Zabalegui LF, Cameron K, Guadagnoli M, Jansen M, Burggraaf M, et al. The TNF family member APRIL promotes colorectal tumorigenesis. Cell Death Differ. 2012;19(11):1826-35.
16. Kimberley FC, Medema JP, Hahne M. APRIL in B-cell malignancies and autoimmunity. Results and problems in cell differentiation. 2009;49:161-82.
17. Endo T, Nishio M, Enzler T, Cottam HB, Fukuda T, James DF, et al. BAFF And APRIL Support Chronic Lymphocytic Leukemia B Cell Survival Through Activation Of The Canonical NF-{kappa}B Pathway. Blood. 2006.
18. Cols M, Barra CM, He B, Puga I, Xu W, Chiu A, et al. Stromal endothelial cells establish a bidirectional crosstalk with chronic lymphocytic leukemia cells through the TNF-related factors BAFF, APRIL, and CD40L. J Immunol. 2012;188(12):6071-83.
19. Kern C, Cornuel JF, Billard C, Tang R, Rouillard D, Stenou V, et al. Involvement of BAFF and APRIL in the resistance to apoptosis of B-CLL through an autocrine pathway. Blood. 2004;103(2):679-88.
20. Planelles L, Carvalho-Pinto CE, Hardenberg G, Smaniotto S, Savino W, Gomez-Caro R, et al. APRIL promotes B-1 cell-associated neoplasm. Cancer Cell. 2004;6(4):399-408.

21. Planelles L, Castillo-Gutierrez S, Medema JP, Morales-Luque A, Merle-Beral H, Hahne M. APRIL but not BLyS serum levels are increased in chronic lymphocytic leukemia: prognostic relevance of APRIL for survival. Haematologica. 2007;92(9):1284-5.
22. Lascano V, Guadagnoli M, Schot JG, Luijks DM, Guikema JE, Cameron K, et al. Chronic lymphocytic leukemia disease progression is accelerated by APRIL-TACI interaction in the TCL1 transgenic mouse model. Blood. 2013;122(24):3960-3.
23. He B, Chadburn A, Jou E, Schattner EJ, Knowles DM, Cerutti A. Lymphoma B cells evade apoptosis through the TNF family members BAFF/BLyS and APRIL. J Immunol. 2004;172(5):3268-79.
24. Schwaller J, Schneider P, Mhawech-Fauceglia P, McKee T, Myit S, Matthes T, et al. Neutrophil-derived APRIL concentrated in tumor lesions by proteoglycans correlates with human B-cell lymphoma aggressiveness. Blood. 2007;109(1):331-8.
25. Bouamar H, Abbas S, Lin AP, Wang L, Jiang D, Holder KN, et al. A capture-sequencing strategy identifies IRF8, EBF1, and APRIL as novel IGH fusion partners in B-cell lymphoma. Blood. 2013;122(5):726-33.
26. Tzankov A, Gschwendtner A, Augustin F, Fiegl M, Obermann EC, Dirnhofer S, et al. Diffuse large B-cell lymphoma with overexpression of cyclin e substantiates poor standard treatment response and inferior outcome. Clin Cancer Res. 2006;12(7 Pt 1):2125-32.
27. Hans CP, Weisenburger DD, Greiner TC, Gascoyne RD, Delabie J, Ott G, et al. Confirmation of the molecular classification of diffuse large B-cell lymphoma by immunohistochemistry using a tissue microarray. Blood. 2004;103(1):275-82.
28. Callanan MB, Le Baccon P, Mossuz P, Duley S, Bastard C, Hamoudi R, et al. The IgG Fc receptor, FcgammaRIIB, is a target for deregulation by chromosomal translocation in malignant lymphoma. Proc Natl Acad Sci U S A. 2000;97(1):309-14.
29. Mestre-Escorihuela C, Rubio-Moscardo F, Richter JA, Siebert R, Climent J, Fresquet V, et al. Homozygous deletions localize novel tumor suppressor genes in B-cell lymphomas. Blood. 2007;109(1):271-80.
30. Borregaard N. Neutrophils, from marrow to microbes. Immunity.33(5):657-70.
31. Matthes T, Dunand-Sauthier I, Santiago-Raber ML, Krause KH, Donze O, Passweg J, et al. Production of the plasma-cell survival factor a proliferation-inducing ligand (APRIL) peaks in myeloid precursor cells from human bone marrow. Blood. 2011;118(7):1838-44.
32. Caronni N, Savino B, Bonecchi R. Myeloid cells in cancer-related inflammation. Immunobiology. 2015;220(2):249-53.
33. Murphy PM, Baggiolini M, Charo IF, Hebert CA, Horuk R, Matsushima K, et al. International union of pharmacology. XXII. Nomenclature for chemokine receptors. Pharmacol Rev. 2000;52(1):145-76.
34. Sugawara T, Miyamoto M, Takayama S, Kato M. Separation of neutrophils from blood in human and laboratory animals and comparison of the chemotaxis. Journal of pharmacological and toxicological methods. 1995;33(2):91-100.
35. Carta S, Tassi S, Semino C, Fossati G, Mascagni P, Dinarello CA, et al. Histone deacetylase inhibitors prevent exocytosis of interleukin-1beta-containing secretory lysosomes: role of microtubules. Blood. 2006;108(5):1618-26.
36. Koyama T, Tsukamoto H, Miyagi Y, Himeji D, Otsuka J, Miyagawa H, et al. Raised serum APRIL levels in patients with systemic lupus erythematosus. Annals of the rheumatic diseases. 2005;64(7):1065-7.

37. Matsushita T, Fujimoto M, Hasegawa M, Tanaka C, Kumada S, Ogawa F, et al. Elevated serum APRIL levels in patients with systemic sclerosis: distinct profiles of systemic sclerosis categorized by APRIL and BAFF. The Journal of rheumatology. 2007;34(10):2056-62.
38. Morel J, Roubille C, Planelles L, Rocha C, Fernandez L, Lukas C, et al. Serum levels of tumour necrosis factor family members a proliferation-inducing ligand (APRIL) and B lymphocyte stimulator (BLyS) are inversely correlated in systemic lupus erythematosus. Annals of the rheumatic diseases. 2009;68(6):997-1002.
39. Jiang Y, Dominguez PM, Melnick AM. The many layers of epigenetic dysfunction in B-cell lymphomas. Current opinion in hematology. 2016;23(4):377-84.
40. Chambwe N, Kormaksson M, Geng H, De S, Michor F, Johnson NA, et al. Variability in DNA methylation defines novel epigenetic subgroups of DLBCL associated with different clinical outcomes. Blood. 2014;123(11):1699-708.
41. Venza I, Visalli M, Fortunato C, Ruggeri M, Ratone S, Caffo M, et al. PGE2 induces interleukin-8 derepression in human astrocytoma through coordinated DNA demethylation and histone hyperacetylation. Epigenetics. 2012;7(11):1315-30.
42. Dominguez PM, Teater M, Chambwe N, Kormaksson M, Redmond D, Ishii J, et al. DNA Methylation Dynamics of Germinal Center B Cells Are Mediated by AID. Cell Rep. 2015;12(12):2086-98.
43. Greeve J, Philipsen A, Krause K, Klapper W, Heidorn K, Castle BE, et al. Expression of activation-induced cytidine deaminase in human B-cell non-Hodgkin lymphomas. Blood. 2003;101(9):3574-80.
44. Lunning MA, Green MR. Mutation of chromatin modifiers; an emerging hallmark of germinal center B-cell lymphomas. Blood Cancer J. 2015;5:e361.
45. Pasqualucci L, Dominguez-Sola D, Chiarenza A, Fabbri G, Grunn A, Trifonov V, et al. Inactivating mutations of acetyltransferase genes in B-cell lymphoma. Nature. 2011;471(7337):189-95.
46. Morin RD, Mendez-Lago M, Mungall AJ, Goya R, Mungall KL, Corbett RD, et al. Frequent mutation of histone-modifying genes in non-Hodgkin lymphoma. Nature. 2011;476(7360):298-303.
47. Tran TH, Nakata M, Suzuki K, Begum NA, Shinkura R, Fagarasan S, et al. B cell-specific and stimulation-responsive enhancers derepress Aicda by overcoming the effects of silencers. Nat Immunol. 2010;11(2):148-54.
48. Bandobashi K, Maeda A, Teramoto N, Nagy N, Szekely L, Taguchi H, et al. Intranuclear localization of the transcription coadaptor CBP/p300 and the transcription factor RBP-Jk in relation to EBNA-2 and -5 in B lymphocytes. Virology. 2001;288(2):275-82.
49. Ansell SM, Stenson M, Habermann TM, Jelinek DF, Witzig TE. Cd4+ T-cell immune response to large B-cell non-Hodgkin's lymphoma predicts patient outcome. J Clin Oncol. 2001;19(3):720-6.
50. Xu Y, Kroft SH, McKenna RW, Aquino DB. Prognostic significance of tumour-infiltrating T lymphocytes and T-cell subsets in de novo diffuse large B-cell lymphoma: a multiparameter flow cytometry study. Br J Haematol. 2001;112(4):945-9.
51. Nakayama S, Yokote T, Hirata Y, Akioka T, Miyoshi T, Hiraoka N, et al. TNF-alpha expression in tumor cells as a novel prognostic marker for diffuse large B-cell lymphoma, not otherwise specified. The American journal of surgical pathology. 2014;38(2):228-34.
52. Huang S, Robinson JB, Deguzman A, Bucana CD, Fidler IJ. Blockade of nuclear factor-kappaB signaling inhibits angiogenesis and tumorigenicity of human ovarian cancer cells by

suppressing expression of vascular endothelial growth factor and interleukin 8. Cancer research. 2000;60(19):5334-9.
53. Inoue K, Slaton JW, Kim SJ, Perrotte P, Eve BY, Bar-Eli M, et al. Interleukin 8 expression regulates tumorigenicity and metastasis in human bladder cancer. Cancer research. 2000;60(8):2290-9.
54. Li A, Varney ML, Singh RK. Expression of interleukin 8 and its receptors in human colon carcinoma cells with different metastatic potentials. Clin Cancer Res. 2001;7(10):3298-304.
55. Murphy C, McGurk M, Pettigrew J, Santinelli A, Mazzucchelli R, Johnston PG, et al. Nonapical and cytoplasmic expression of interleukin-8, CXCR1, and CXCR2 correlates with cell proliferation and microvessel density in prostate cancer. Clin Cancer Res. 2005;11(11):4117-27.
56. Campbell LM, Maxwell PJ, Waugh DJ. Rationale and Means to Target Pro-Inflammatory Interleukin-8 (CXCL8) Signaling in Cancer. Pharmaceuticals. 2013;6(8):929-59.
57. Gregoire M, Guilloton F, Pangault C, Mourcin F, Sok P, Latour M, et al. Neutrophils trigger a NF-kappaB dependent polarization of tumor-supportive stromal cells in germinal center B-cell lymphomas. Oncotarget. 2015;6(18):16471-87.
58. Fujii A, Ohshima K, Hamasaki M, Makimoto Y, Haraoka S, Utsunomiya H, et al. Differential expression of chemokines, chemokine receptors, cytokines and cytokine receptors in diffuse large B cell malignant lymphoma. Int J Oncol. 2004;24(3):529-38.
59. Nacinovic-Duletic A, Stifter S, Dvornik S, Skunca Z, Jonjic N. Correlation of serum IL-6, IL-8 and IL-10 levels with clinicopathological features and prognosis in patients with diffuse large B-cell lymphoma. Int J Lab Hematol. 2008;30(3):230-9.

LEGEND TO FIGURES

Figure 1: blood neutrophils constitutively produce APRIL

A) qRT-PCR analysis for APRIL mRNA in FACS-sorted mature BM and blood neutrophils. A value of one was arbitrarily given to mature BM neutrophils (left panel). Data are representative of three healthy donors. PBLs from healthy donors were surface-stained for CD13 and CD16, and for APRIL-production after cell permeabilization (middle panel). Overlaid histogram plots for gated $CD13^{+}CD16^{+}$ neutrophils are shown. Grey and black lines correspond to control Ig and Stalk-1 staining, respectively. Data are representative of at least twenty healthy donors. ELISA for APRIL in the supernatant of 24hr culture from unstimulated neutrophils (right panel). Data are representative of three donors. B) H_2O_2 production in unstimulated (NS) and stimulated neutrophils with PMA, TNF and fMLP (top left panel). Data show maximum relative light units (RLU) observed during a period of 10 min. APRIL mRNA expression level at 6 and 12 h was analysed by qRT-PCR (top right panel). Data were normalized using actin mRNA expression and are presented as fold increases compared to unstimulated conditions. Secreted APRIL was analysed by ELISA in culture supernatants at the indicated time points (bottom panel). Fold

increases compared to unstimulated conditions are shown. Data are representative of three healthy donors. *P<0.05.

Figure 2: DLBCL tumor cells constitutively produce CXCL-8

A) DLBCL biopsies were selected according to the level of APRIL expression (Stalk-1 staining, upper panel). APRIL-producing (Stalk-1 staining, green) neutrophils were identified by Elastase staining (red) (middle panel). The merge picture also shows Hoechst nuclear staining (blue). Scale bar = 10μm. Lysates of APRIL^{neg} and APRIL^{high} DLBCL biopsies were profiled for chemokine expression (bottom left panel). Dots corresponding to CXCL-8 are arrowed. Dots corresponding to other neutrophil-acting chemokines present on the blot are also indicated. B) CXCL-8 protein was quantified in lysates of the indicated DLBCL biopsies by ELISA. C) *In situ* CXCL-8 staining of the indicated biopsies. Figure is representative of a total of 101 patients. Scale bar = 20 μm. D) *In situ* fluorescence costaining of the indicated DLBCL biopsies for CD20 (green) and CXCL-8 (red). Hoechst nuclear staining is also shown (blue). Figure is representative of three patients for each case. Scale bar = 20 μm. E) CXCL-8 mRNA expression in CD20$^+$ and CD20$^-$ fraction of primary DLBCL cells. F) CXCL-8 concentration in the supernatant of unstimulated, anti-BCR/CD40L, and TNF-stimulated DLBCL cells lines. Figure is representative of at least five experiments. *P<0.05.

Figure 3: *in vitro* chemotactic activity of CXCL-8$^+$ DLBCL tumor cells for neutrophils

A) Chemoattraction of purified human blood neutrophils by DLBCL cell lines. B) Chemoattraction by the DLBCL cell line OCI-Ly18 in the presence of an anti-CXCL-8 or control antibody (cIg). The figure is representative of three experiments. The fold increase compared to medium alone is shown. C) Surface expression of the indicated chemokine receptors on CD13$^+$CD16$^+$ gated blood neutrophils from healthy donors. Grey lines correspond to control Ig staining. Results are representative of at least three healthy donors.

Figure 4: *in vivo* chemotactic activity of CXCL-8$^+$ DLBCL tumor cells for neutrophils

A) Bone marrow cells from humanized NOG mice were surface stained for human CD13, CD16 and CD45, and for APRIL-production after cell permeabilization. Grey and black lines correspond to control Ig and Stalk-1 staining, respectively. B) Biopsies of the indicated DLBCL

cell lines xenografted in NOG mice were stained for neutrophils (Elastase) and APRIL-producing cells (Stalk-1). Scale bar = 50 µm. C) Fluorescence costaining of a OCI-Ly18 biopsy for APRIL-producing cells (Stalk-1, red) and neutrophils (Elastase, green). The merge picture also shows Hoechst nuclear staining (blue). Scale bar = 20 µm. Results are representative of at least three different mice.

Figure 5: Heterogeneous phenotypes for CXCL-8$^+$ DLBCL tumor cells

A) CXCL-8$^+$ DLBCL cell lines were analysed by flow cytometry for the indicated surface markers. Bcl-2 expression was analysed after cell permeabilization. Histogram plots are shown. B) CXCL-8 mRNA expression in the control OCI-Ly18 DLBCL cell line and purified naïve, GC and memory B cells from tonsils. Figure is representative of three tonsillitis patients

Figure 6: epigenetic regulation of CXCL-8 expression in DLBCL

A) qRT-PCR analysis for CXCL-8 mRNA in DLBCL cell lines treated with TSA, decitabine or DMSO vehicle control. Data are representative of three experiments, **P*<0.05 *vs* DMSO-treated group. B) CXCL-8 concentration in the supernatant of cell lines treated with TSA, Decitabine or DMSO vehicle control. **P*<0.05 *vs* DMSO treated

Figure 1

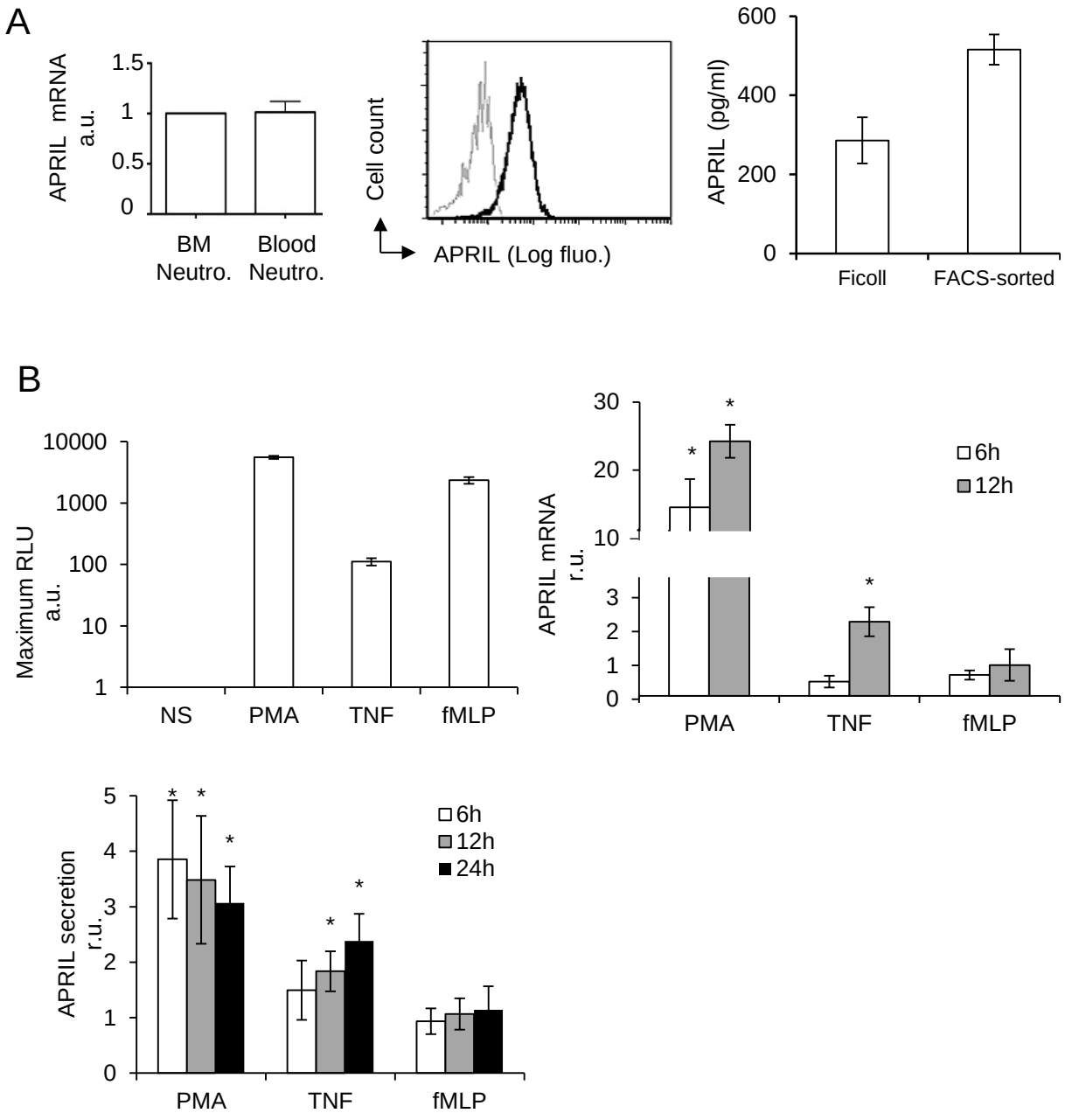
A
APRIL mRNA a.u.
1.5
1
0.5
0
BM Neutro.
Blood Neutro.
Cell count
APRIL (Log fluo.)
APRIL (pg/ml)
600
400
200
0
Ficoll
FACS-sorted
B
Maximum RLU a.u.
10000
1000
100
10
1
NS
PMA
TNF
fMLP
APRIL mRNA r.u.
30
20
10
3
2
1
0
6h
12h
PMA
TNF
fMLP
APRIL secretion r.u.
5
4
3
2
1
0
6h
12h
24h
PMA
TNF
fMLP

Figure 2

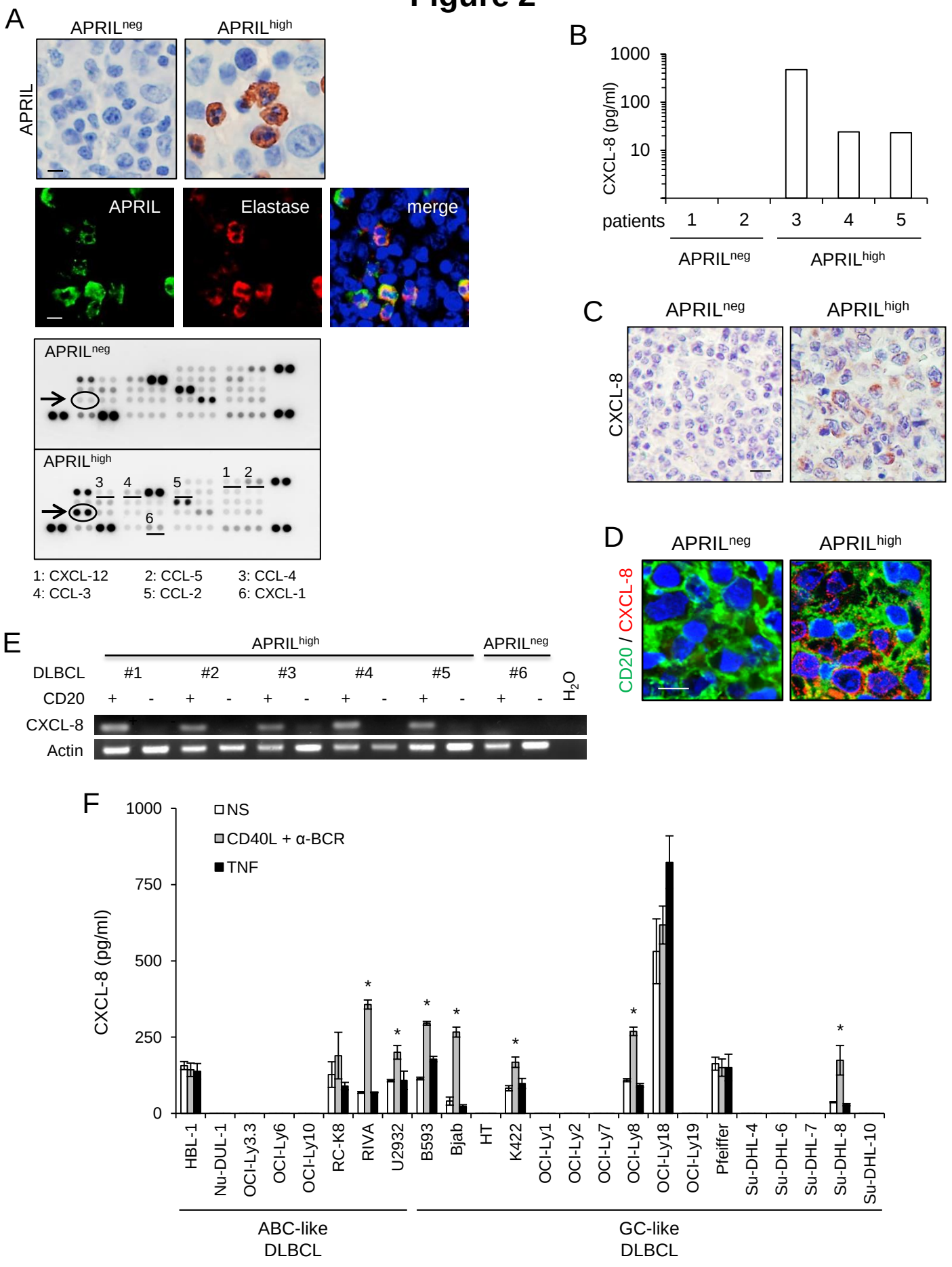
A
APRIL^neg
APRIL^high
APRIL
APRIL
Elastase
merge
APRIL^neg
APRIL^high
1: CXCL-12
2: CCL-5
3: CCL-4
4: CCL-3
5: CCL-2
6: CXCL-1
B
1000
100
10
CXCL-8 (pg/ml)
patients 1 2 3 4 5
APRIL^neg
APRIL^high
C
APRIL^neg
APRIL^high
CXCL-8
D
APRIL^neg
APRIL^high
CD20 / CXCL-8
E
APRIL^high
APRIL^neg
DLBCL #1 #2 #3 #4 #5 #6
CD20 + - + - + - + - + - + -
H2O
CXCL-8
Actin
F
NS
CD40L + α-BCR
TNF
CXCL-8 (pg/ml)
1000
750
500
250
0
HBL-1
Nu-DUL-1
OCI-Ly3.3
OCI-Ly6
OCI-Ly10
RC-K8
RIVA
U2932
B593
Bjab
HT
K422
OCI-Ly1
OCI-Ly2
OCI-Ly7
OCI-Ly8
OCI-Ly18
OCI-Ly19
Pfeiffer
Su-DHL-4
Su-DHL-6
Su-DHL-7
Su-DHL-8
Su-DHL-10
ABC-like DLBCL
GC-like DLBCL

Figure 3

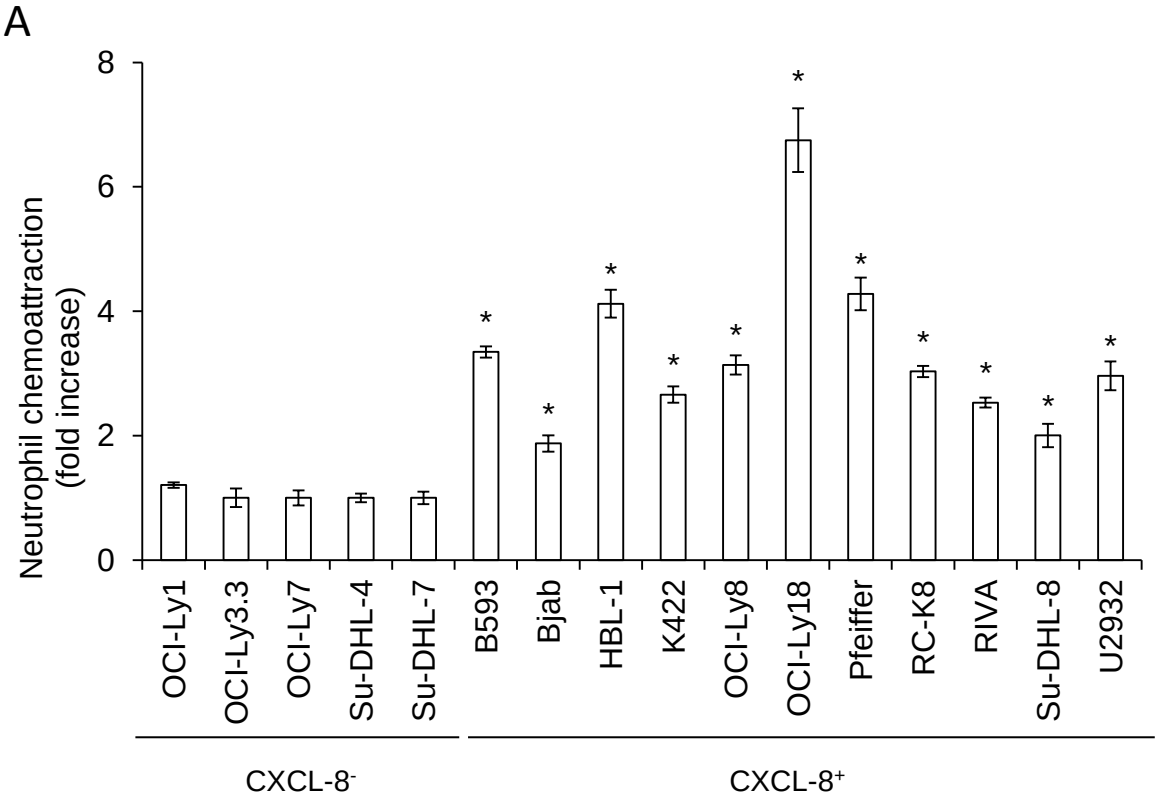
A
Neutrophil chemoattraction (fold increase)
0
2
4
6
8
OCI-Ly1
OCI-Ly3.3
OCI-Ly7
Su-DHL-4
Su-DHL-7
B593
Bjab
HBL-1
K422
OCI-Ly8
OCI-Ly18
Pfeiffer
RC-K8
RIVA
Su-DHL-8
U2932
CXCL-8-
CXCL-8+

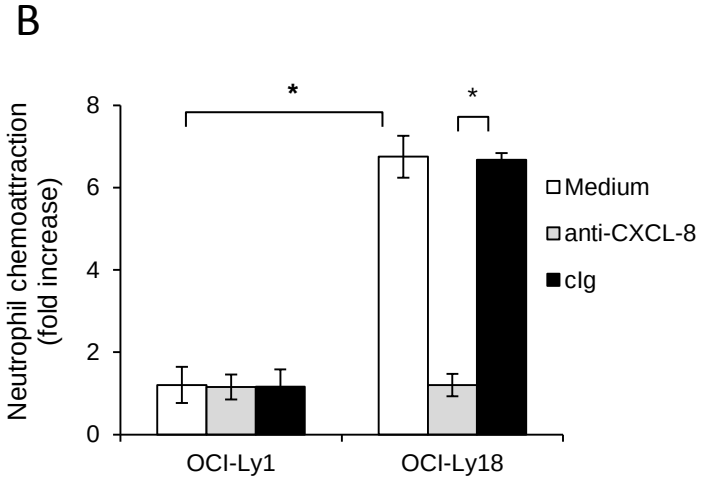
B
Neutrophil chemoattraction (fold increase)
0
2
4
6
8
Medium
anti-CXCL-8
clg
OCI-Ly1
OCI-Ly18

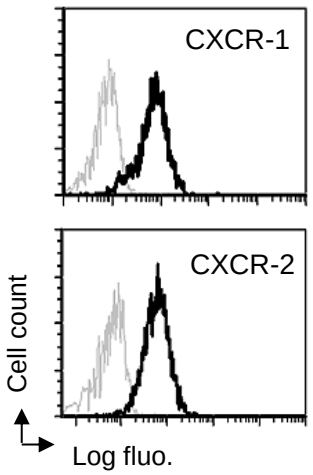
C
CXCR-1
CXCR-2
Cell count
Log fluo.

Figure 4

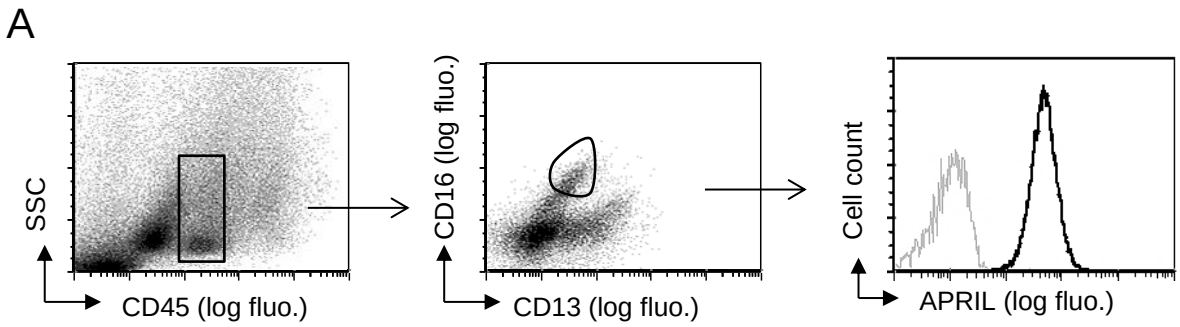
A
SSC
CD45 (log fluo.)
CD16 (log fluo.)
CD13 (log fluo.)
Cell count
APRIL (log fluo.)

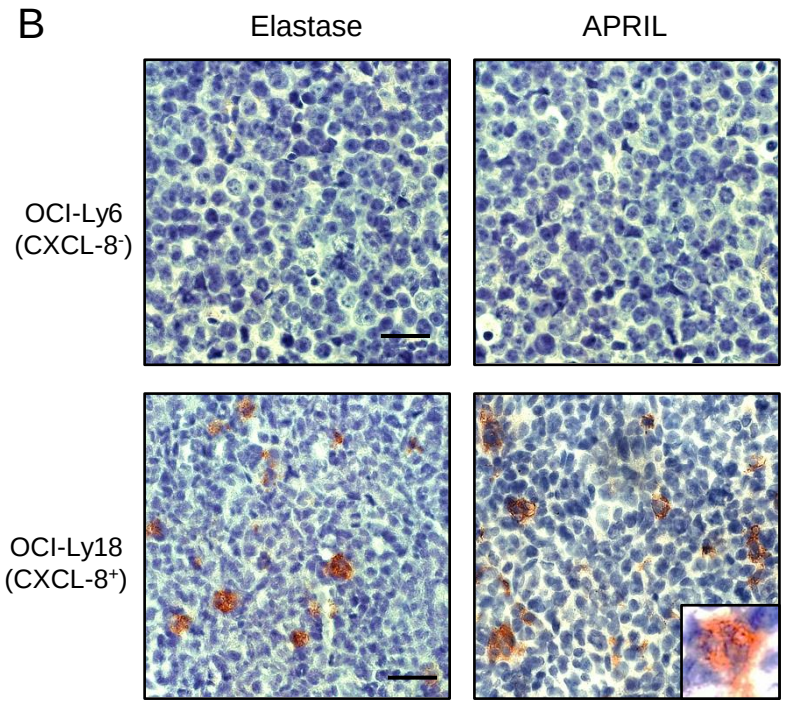
B
Elastase
APRIL
OCI-Ly6
(CXCL-8-)
OCI-Ly18
(CXCL-8+)

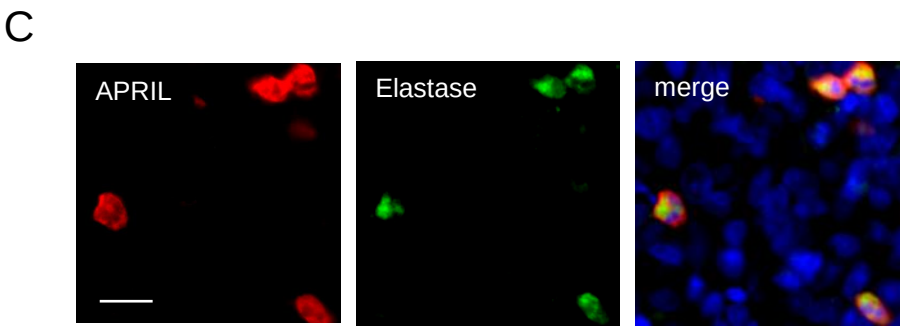
C
APRIL
Elastase
merge

Figure 5

A

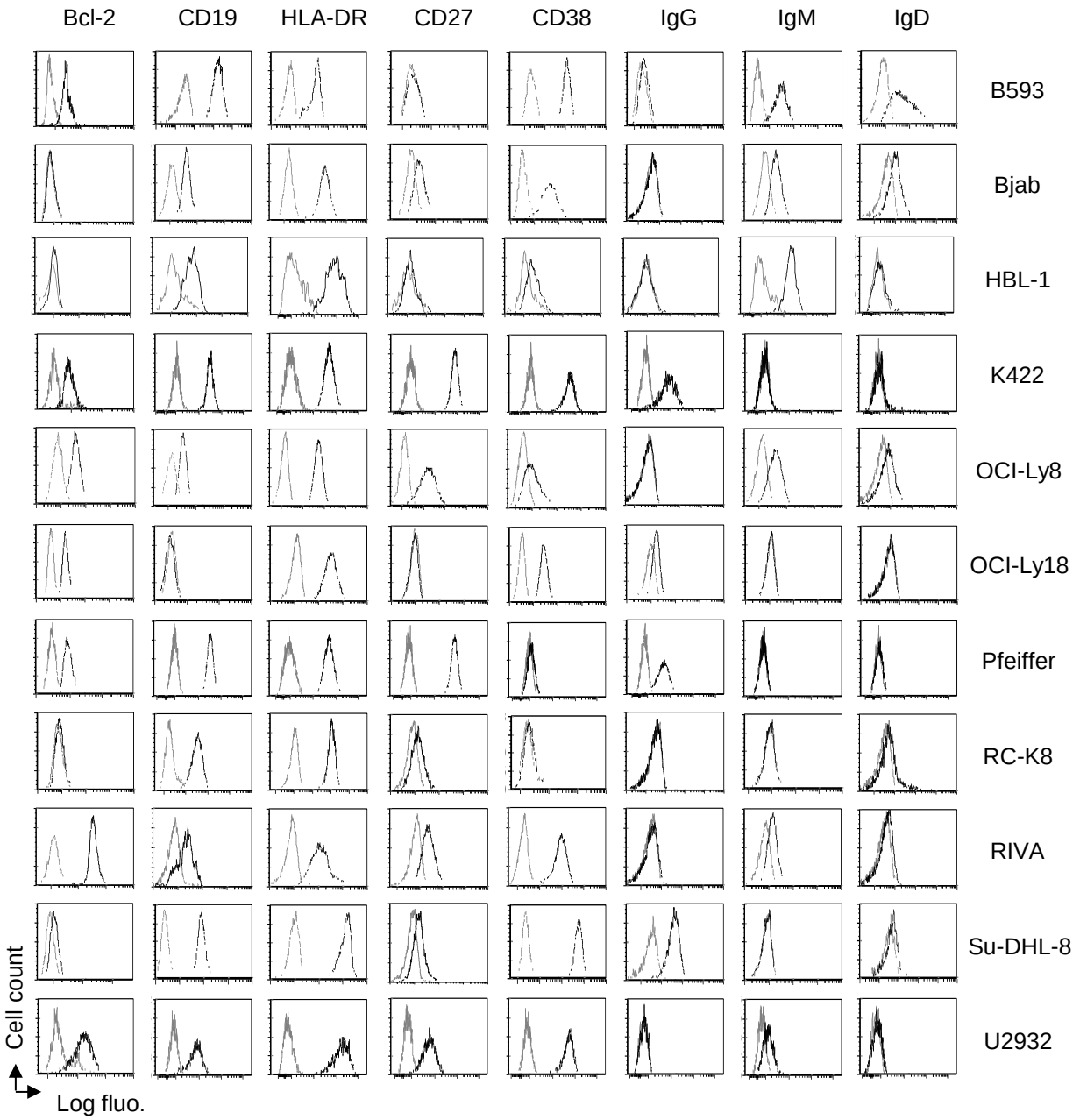
Bcl-2
CD19
HLA-DR
CD27
CD38
IgG
IgM
IgD
B593
Bjab
HBL-1
K422
OCI-Ly8
OCI-Ly18
Pfeiffer
RC-K8
RIVA
Su-DHL-8
U2932
Cell count
Log fluo.

B

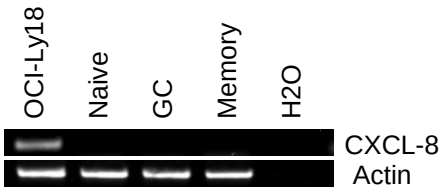
OCI-Ly18
Naive
GC
Memory
H2O
CXCL-8
Actin

Figure 6

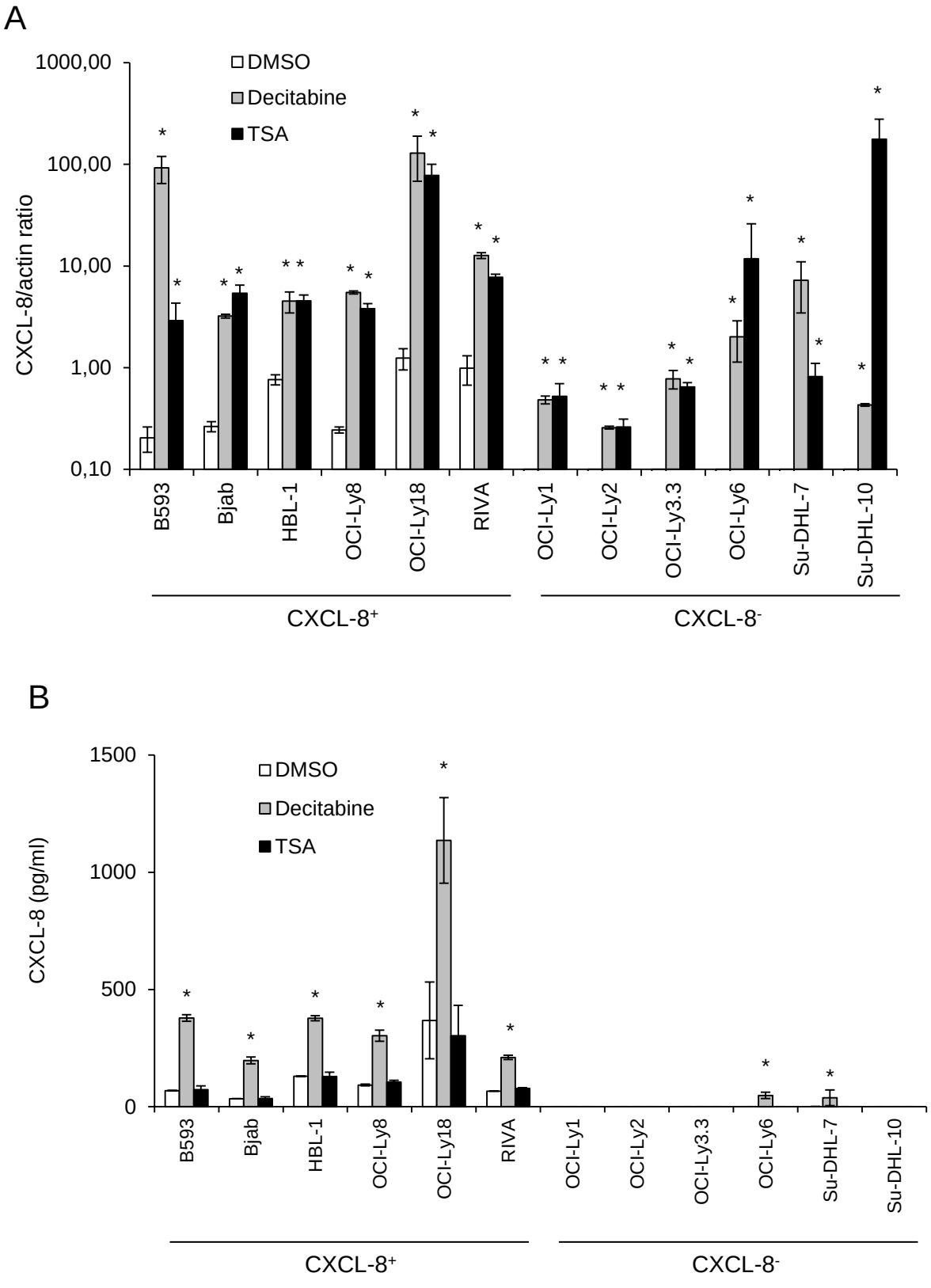
A
1000,00
100,00
10,00
1,00
0,10
CXCL-8/actin ratio
DMSO
Decitabine
TSA
B593
Bjab
HBL-1
OCI-Ly8
OCI-Ly18
RIVA
OCI-Ly1
OCI-Ly2
OCI-Ly3.3
OCI-Ly6
Su-DHL-7
Su-DHL-10
CXCL-8+
CXCL-8-
B
1500
1000
500
0
CXCL-8 (pg/ml)
DMSO
Decitabine
TSA
B593
Bjab
HBL-1
OCI-Ly8
OCI-Ly18
RIVA
OCI-Ly1
OCI-Ly2
OCI-Ly3.3
OCI-Ly6
Su-DHL-7
Su-DHL-10
CXCL-8+
CXCL-8-

Figure 1 sup

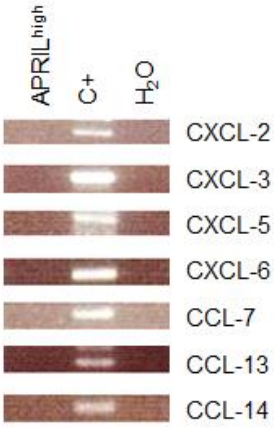

CXCL-8 is the unique neutrophil chemokine detectable in DLBCL biopsies
RT-PCR analysis for the indicated neutrophil-specific chemokines. Positive control for CXCL-2, -6, -7, CCL-7 and CXCL-3, -5, CCL-13, -14 was total PBL and tonsil mRNA, respectively.

Figure 2 sup

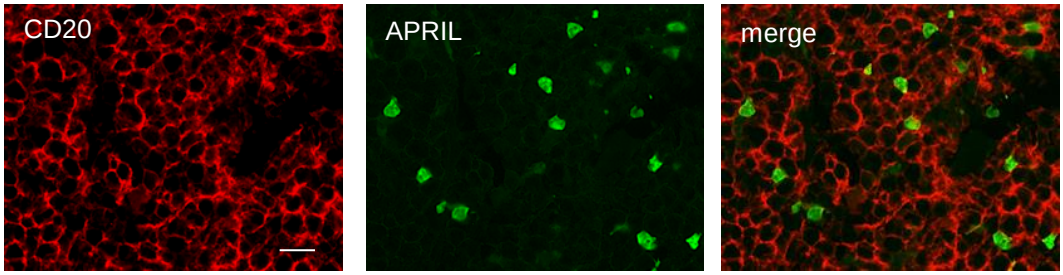

APRIL-producing neutrophils infiltrate the tumor nest
Costaining for CD20 (red) and APRIL-producing cells (Stalk-1, green). Scale bar = 20 µm.

Figure 3 sup

A

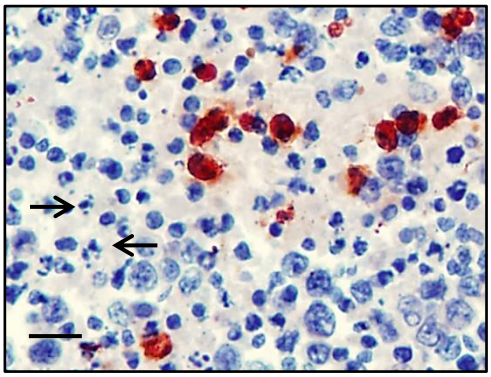

B

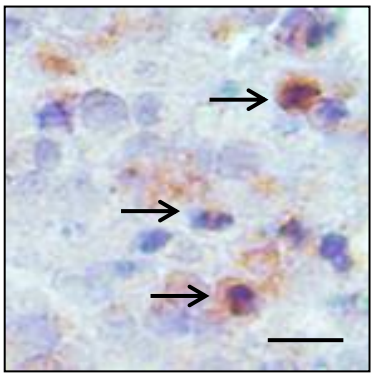

CXCL-8+ neutrophils are present in DLBCL necrotic tumors
A) APRIL immunostaining of neutrophils from a DLBCL biopsy with necrosis. Necrotic cells with pycnotic nuclei are arrowed . Figure is representative of 30 cases. B) CXCL-8 immunostaining of a DLBCL biopsy associated with necrosis. CXCL-8+ neutrophils with polymorph nuclei are arrowed. Figure is representative of 12 cases. Scale bar = 20 µm.

Figure 4 sup

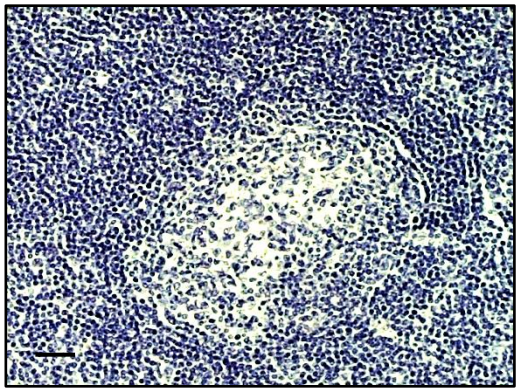

Healthy B-cells are CXCL-8 negative
In situ CXCL-8 staining of a human tonsil GC. Figure is representative of five tonsillitis patients. Scale bar = 100 µm.